

Numerical Investigation of Cavitation Bubble Collapsing Behavior

Byeong Rog Shin¹

¹Department of Mechanical Engineering, Changwon National University,
Changwon 641-773, Korea: brshin@changwon.ac.kr

ABSTRACT

A preconditioned numerical method for cavitating flow is applied to solve shock-cavitation bubble interaction problems. The present method employs a finite-difference Runge-Kutta method and Roe's flux difference splitting approximation with the MUSCL-TVD scheme. A homogeneous equilibrium gas-liquid multi-phase model taken account of the compressibility of mixed media is used. Therefore, the present density-based numerical method permits simple treatment of the whole gas-liquid mixed flow field, including wave propagation, large density changes and incompressible flow characteristics at low Mach number. By applying this method, firstly a Riemann problem for Euler equations of one dimensional shock tube was computed for validation. Then, shock-bubble interaction problems between cylindrical bubbles located in the liquid and incident liquid shock wave are computed. Bubble collapsing behavior, shock-bubble interaction and shock transmission/reflection pattern are investigated.

Keywords

Homogeneous Cavitation Model, Equation of State, Shock-Bubble Interaction, Bubble Collapsing, Riemann Problem.

1 INTRODUCTION

Cavitation is well encountered a phase change phenomenon in the flow of hydrofoils, rocket engine turbopumps, marine propellers and under water vehicles with a high-speed in working fluid of liquid state. When cavitation occurs and collapses near solid surfaces, it causes the noise, vibration and damage to hydraulic machine systems (Brennen 1995). In the sense of reducing these unfavorable effects, therefore, technology of accurate prediction/estimation of cavitation to investigate the bubble collapsing mechanism are very important in development of these fluid devices.

To understand the behavior of collapsing of cavitation bubbles, some efforts to propose cavity flow model for numerical simulations (Chen & Heister 1994, Deshpande

et al 1997, Singhal et al 1997, Merkle et al 1998, Kunz et al 2000) and, analytical and experimental method for shock-bubble interaction problems (Bourne N.K & Field 1992, Takahira et al 1994, Tomita & Shima 1986) have been made. Recently, present author has proposed a mathematical cavity flow model (Shin et al 2003, Shin & Ikohagi 1999, Shin 2001, Yamamoto & Shin 2004) based on a homogeneous equilibrium model taking account of the compressibility of the gas-liquid two-phase media. With this model, the mechanism of developing cavitation has been investigated through the application to a couple of cavitating flows around a hydrofoil (Iga et al 2003, Shin et al 2004, Shin & Yamamoto 2005).

The purpose of this paper is to extend to a shock-bubble interaction problem with a high-order Runge-Kutta method and MUSCL TVD solution method for stable and accurate treatment of gas-liquid interfaces considered by contact discontinuity. As numerical examples, one-dimensional (1-D) gas-liquid two-phase shock tube problems are computed to investigate detailed unsteady shock wave phenomena including the propagation of both compression and expansion waves. And then, numerical investigation for shock-bubble interaction problems between cylindrical cavitation bubbles located in the liquid and incident liquid shock wave are solved.

2 HOMOGENEOUS CAVITATION MODEL

Gas-liquid two-phase flow of cavity flow is possible to model into an pseudo single-phase flow by using concept of the homogeneous equilibrium model (Shin et al 2003) in which thermodynamic equilibrium is assumed and velocity slip between both phases is neglected.

Under this model concept, the pressure for gas-liquid two-phase media is determined by using a combination of two equations of state for gas phase and liquid phase, that is written as follows:

$$\rho = \frac{p(p + p_c)}{K(1-Y)p(T + T_c) + RY(p + p_c)T} \quad (1)$$

where, ρ, p, Y and T are the mixture density, pressure, quality of vapor and the temperature, respectively. R is the gas constant and K, p_c and T_c represent the liquid constant, pressure constant and the temperature constant for water, respectively. This equation is derived from the local equilibrium assumption, and corresponds to the equations of state for pure liquid ($Y=0$) by Tammann (Chen & Collins 1971) and ideal gas ($Y=1$), respectively. Therefore, the apparent compressibility is considered, and the speed of sound c is exactly derived by using thermodynamic relations as

$$c^2 = \rho C_p \left(\frac{\partial \rho}{\partial T} + \rho C_p \frac{\partial \rho}{\partial p} \right)^{-1} \quad (2)$$

C_p is the specific heat capacity at constant pressure of $C_p = Y C_{pg} + (1-Y) C_{pl}$. Subscripts l and g mean liquid phase and gas phase. The relation between the local void fraction α and the quality Y is given as $\rho(1-Y) = (1-\alpha)\rho_l$ and $\rho Y = \alpha\rho_g$.

3 NUMERICAL METHOD

3.1 Fundamental Equations

Based on the cavitation model concept described in the previous Chapter and neglecting the surface tension, the 2-D governing equations for the mixture mass, momentum, energy and the gas-phase mass conservation can be written in the curvilinear coordinates (ξ, η) as follows:

$$\frac{\partial \mathbf{Q}}{\partial t} + \frac{\partial \mathbf{E}}{\partial \xi} + \frac{\partial \mathbf{F}}{\partial \eta} = \frac{\partial \mathbf{E}_v}{\partial \xi} + \frac{\partial \mathbf{F}_v}{\partial \eta} + \mathbf{S} \quad (3)$$

where \mathbf{Q} is an unknown variable vector, \mathbf{E}, \mathbf{F} are flux vectors and $\mathbf{E}_v, \mathbf{F}_v$ are viscous terms. \mathbf{S} is the source term of $[0, 0, 0, 0, S_e - S_c]^T$. For instance, \mathbf{Q}, \mathbf{E} and \mathbf{E}_v are,

$$\mathbf{Q} = J \begin{pmatrix} \rho \\ \rho u \\ \rho v \\ e \\ \rho Y \end{pmatrix}, \quad \mathbf{E} = J \begin{pmatrix} \rho U \\ \rho u U + \xi_x p \\ \rho v U + \xi_y p \\ \rho U H \\ \rho U Y \end{pmatrix}$$

$$\mathbf{E}_v = J \begin{pmatrix} 0 \\ \xi_x \tau_{xx} + \xi_y \tau_{xx} \\ \xi_x \tau_{yx} + \xi_y \tau_{yy} \\ \xi_x T_{11} + \xi_y T_{22} \\ \xi_x \Re Y_x + \xi_y \Re Y_y \end{pmatrix}$$

where the Jacobian J of the transformation from Cartesian coordinates x_i to general curvilinear coordinates ξ_i . The relationships between the physical velocity u_i in x_i space and the contravariant velocity U_i in ξ_i space are $U_i = (\partial \xi_i / \partial x_j) u_j$ and $u_i = (\partial x_i / \partial \xi_j) U_j$ respectively,

using the summation convention. $T_{11} = u \tau_{xx} + v \tau_{xy} + \kappa \partial T / \partial x$, $T_{22} = u \tau_{yx} + v \tau_{yy} + \kappa \partial T / \partial y$ and κ is the coefficient of thermal conductivity. Also, \Re is the effective exchange coefficient, S_e is the rate of evaporation and S_c is the rate of condensation.

The stress tensor τ , the mixture density ρ and the mixture viscosity μ (Beattie & Whally 1982) can be expressed as

$$\tau_{xx} = \frac{2}{3} \mu \left(2 \frac{\partial u}{\partial x} - \frac{\partial v}{\partial y} \right), \tau_{yy} = \frac{2}{3} \mu \left(2 \frac{\partial v}{\partial y} - \frac{\partial u}{\partial x} \right),$$

$$\tau_{xy} = \tau_{yx} = \mu \left(\frac{\partial u}{\partial y} - \frac{\partial v}{\partial x} \right), \rho = (1-\alpha)\rho_l + \alpha\rho_g$$

$$\mu = (1-\alpha)(1+2.5\alpha)\mu_l + \alpha\mu_g$$

H in Eq.(3) is the enthalpy defined by total energy $e = \rho H - p$.

3.2 Preconditioning Formulation

The hydraulic flow with hydraulic transients and hydroacoustics such as cavitating flow has compressible flow characteristic at low Mach number. For this kind of flow, a compressible flow model that includes a preconditioning method is advantageous.

Applying the preconditioning method to Eq.(3), we obtain 2-D preconditioned governing equations with unknown variable vectors $\mathbf{W} = [p, u, v, T, Y]^T$ written in curvilinear coordinates as follows (Shin et al 2004):

$$\Gamma^{-1} \frac{\partial \mathbf{W}}{\partial \tau} + \Gamma_w^{-1} \frac{\partial \mathbf{W}}{\partial t} + \frac{\partial (\mathbf{E} - \mathbf{E}_v)}{\partial \xi} + \frac{\partial (\mathbf{F} - \mathbf{F}_v)}{\partial \eta} = \mathbf{S} \quad (4)$$

In this study, τ is pseudo-time and Γ_w^{-1} is a transform matrix of the Jacobian matrix. The preconditioning matrix Γ^{-1} is formed by the addition of the vector $\theta [1, u, v, H, Y]^T$ to the first column of the Γ_w^{-1} (Shin et al 2004).

3.3 Numerical Method

Fundamental equations (3) and (4) are solved by using appropriate numerical methods such as finite-difference method with TVD Runge-Kutta method. For example, the preconditioned governing equations (4) are numerically integrated using the three-point backward finite-difference method of the dual time-stepping integration procedure. Then, Roe's flux difference splitting (FDS) method (Roe 1981) with the MUSCL-TVD scheme (van Leer 1979) is applied to enhance the numerical stability, especially for steep gradients in density and pressure near the gas-liquid interface. Therefore, the derivative of the flux vector, for instance, \mathbf{E} with respect to ξ at point i can be written with the numerical flux as $(\partial \mathbf{E} / \partial \xi) = (\mathbf{E}_{i+1/2} - \mathbf{E}_{i-1/2}) / \Delta \xi$ and then, the approximate Riemann solver based on the Roe's FDS is applied. Hence, the numerical flux $\mathbf{E}_{i+1/2}$ is written as

$$\mathbf{E}_{i+1/2} = \frac{1}{2} \{ \mathbf{E}(\mathbf{Q}_{i+1/2}^L + \mathbf{Q}_{i+1/2}^R) - Z_{i+1/2}^{-1} (\mathbf{L}_p^{-1} | \Lambda | \mathbf{L}_p)_{i+1/2} (\mathbf{W}_{i+1/2}^R - \mathbf{W}_{i+1/2}^L) \} \quad (5)$$

where, Λ is the diagonal matrix of eigenvalues and \mathbf{L}_p and \mathbf{L}_p^{-1} are the left eigenvectors of $Z\partial\mathbf{E}/\partial\mathbf{W}$. $\mathbf{W}_{i+1/2}^{L,R}$ is obtained by applying the third-order MUSCL-TVD scheme as

$$\begin{aligned} \mathbf{W}_{i+1/2}^L &= \mathbf{W}_i + (\phi/4) \\ \{(1-\kappa)D^+ \mathbf{W}_{i-1/2} + (1+\kappa)D^- \mathbf{W}_{i+1/2}\} \\ \mathbf{W}_{i+1/2}^R &= \mathbf{W}_{i+1} - (\phi/4) \\ \{(1-\kappa)D^- \mathbf{W}_{i+3/2} + (1+\kappa)D^+ \mathbf{W}_{i+1/2}\} \end{aligned} \quad (6)$$

Here, the flux-limited values of DW and the minmod function are determined by

$$\begin{aligned} D^+ \mathbf{W}_{i-1/2} &= \min\text{mod}(\delta\mathbf{W}_{i-1/2}, b\delta\mathbf{W}_{i+1/2}), \\ D^- \mathbf{W}_{i+1/2} &= \min\text{mod}(\delta\mathbf{W}_{i+1/2}, b\delta\mathbf{W}_{i-1/2}), \\ \delta\mathbf{W}_{i+1/2} &= \mathbf{W}_{i+1} - \mathbf{W}_i \\ \min\text{mod}(x, y) &= \text{sign}(x) \\ &\max[0, \min\{|x|, y\text{sign}(x)\}] \end{aligned}$$

The linear combination parameter κ is determined by the range of $-1 \leq \kappa \leq 1$ and has an effect on the accuracy. On the other hand, the slope of the flux in the minmod function is controlled by the limiter b . The range of b , $1 \leq b \leq (3-\kappa)/(1-\kappa)$, is determined by the condition of TVD stability.

In the numerical integration of governing equations (4), the 4th-order TVD Runge-Kutta explicit method written followings is used.

$$\begin{aligned} \mathbf{W}^{(1)} &= \mathbf{W}^n - \frac{1}{4} \Delta t \Gamma \mathbf{L}(\mathbf{Q}^n) \\ \mathbf{W}^{(2)} &= \mathbf{W}^n - \frac{1}{3} \Delta t \Gamma \mathbf{L}(\mathbf{Q}^{(1)}) \\ \mathbf{W}^{(3)} &= \mathbf{W}^n - \frac{1}{2} \Delta t \Gamma \mathbf{L}(\mathbf{Q}^{(2)}) \\ \mathbf{W}^{n+1} &= \mathbf{W}^n - \Delta t \Gamma \mathbf{L}(\mathbf{Q}^{(3)}) \end{aligned}$$

where,

$$\mathbf{L}(\mathbf{Q}) = \frac{\partial(\mathbf{E} - \mathbf{E}_v)}{\partial \xi} + \frac{\partial(\mathbf{F} - \mathbf{F}_v)}{\partial \eta} - \mathbf{S}$$

4 NUMERICAL RESULTS

At first, the present computational method has been validated by using the Riemann problem suggested by Sod (Laney 1998) as a standard test problem. The domain is $x[-10 \text{ m}, 10\text{m}]$. In this case Eq. (4) is reduced to 1-D Euler equation without preconditioning. Initial conditions

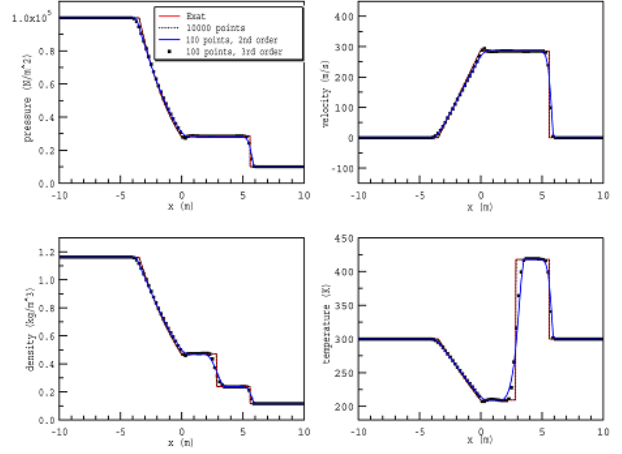


Figure 1 Computational results of pressure, density, velocity and temperature distribution for ideal gas at $\alpha_i=100\%$, time $t=0.01\text{s}$.

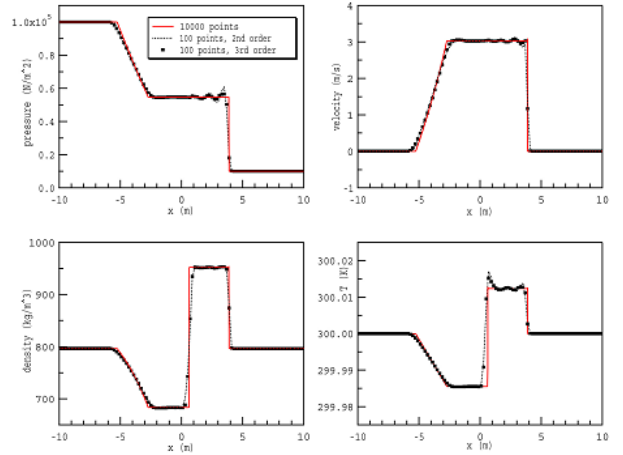


Figure 2 Computational results of pressure, density, velocity and temperature distribution for ideal gas at $\alpha_i=20\%$, time $t=0.21\text{s}$.

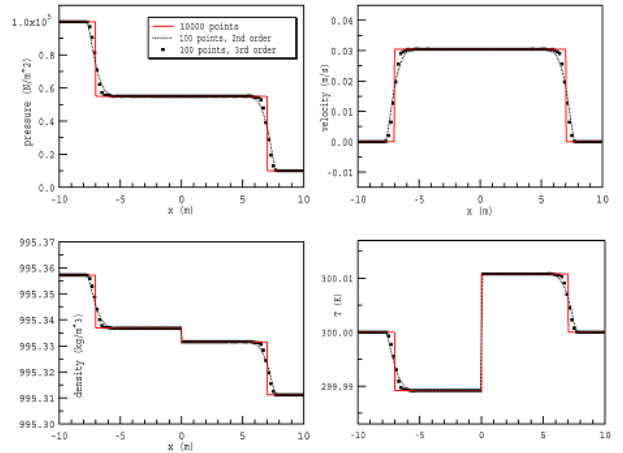


Figure 3 Computational results of pressure, density, velocity and temperature distribution for ideal gas at $\alpha_i=0\%$, time $t=0.00473\text{s}$.

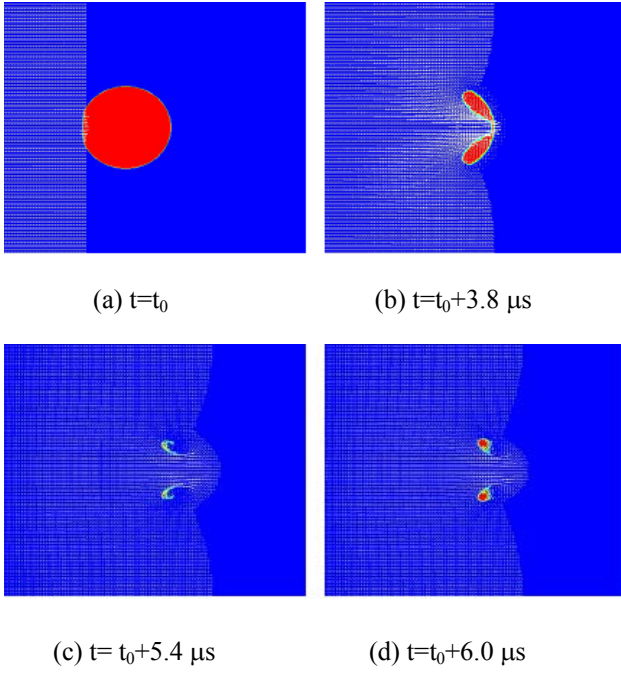


Figure 4 Time evolution of velocity vectors and void fraction distribution (red: $\alpha=1$, blue: $\alpha=0$.)

of left (L)- and right (R)-hand side at discontinuous surface ($x=0$ m) at $T=300K$ are as followings.

$$p_L=0.1\text{MPa}, u_L=0\text{m/s}, \alpha_L=\alpha_i$$

$$p_R=0.1\text{MPa}, u_R=0\text{m/s}, \alpha_R=\alpha_i$$

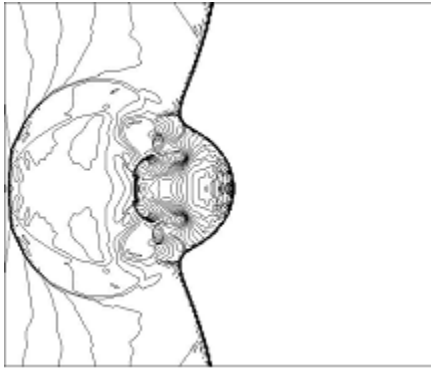


Figure 5 Instantaneous pressure distribution at $t=t_0+5.4\mu\text{s}$

Figure 1 shows comparisons with exact solution for shock tube problem of ideal gas ($\alpha =100\%$) with the ratio of specific heats $\gamma=1.4$ at $t=0.01\text{s}$. The results obtained by present high-order numerical method for gas-liquid two-phase flow with grid points of 10000 are almost coincide with exact solutions (John 1984). The result by 100 points is also fairly well predicted except small dissipation at discontinuity. In this figure symbols represent computed results on the real grid points obtained by third-order MUSCL TVD scheme. Results by both second-order and third-order show a monotonic solution without numerical

oscillation. But, third-order is closer to the exact solution than the second-order even they have same grid points of 100.

Next, based on the validity of the present method, the present high-order method was applied to compressible gas-liquid two-phase shock tube flow in thermal process with arbitrary void fraction to investigate the characteristics of pressure waves propagating in the gas-liquid two-phase medium.

Figure 2 shows calculated results for gas-liquid two-phase medium at void fraction of 20%. In this case compression wave is propagating with decreasing the void fraction because the compression wave compresses the two-phase medium. However expansion wave shows the opposite behavior with increasing the void fraction, resulting the contact discontinuity exists and propagates toward right-hand side by the wave induced velocity. According to the present investigation, induced velocity showed a tendency of increasing at large void fraction. Also, pressure behind the shock wave is higher than single-phase of gas. The third-order scheme is predicted greatly well with very small numerical dissipation and oscillation comparing with the second-order especially at the contact discontinuity.

It means the application of high resolution scheme to present method is advantageous to solve complex flows with gas-liquid interfaces treated by contact discontinuity.

Figure 3 shows another computational results for liquid phase at $\alpha = 0\%$. The expansion wave is propagating like a compression wave. It is different from the gas phase because there exists big difference of speed of sound between gas states and liquid states, and of wave induced velocity. Changes of density and velocity are very small.

Next, present numerical method applied to shock-bubble interaction problems between incident liquid shock wave and cylindrical cavitation bubbles located in the liquid. A square domain with a base of 4 times of bubble diameter (d) and 401 x 401 grid points are used. As an initial condition, a single bubble with void fraction of $\alpha=1$ is located in the center of a stationary flow field with $\alpha=0$ at isothermal condition. In the flow field with uniform pressure of 0.1MPa incident liquid shock wave with a high pressure of 100MPa was placed at $3d$ upstream from single bubble center.

Figure 4 shows Time evolution of velocity vectors and void fraction distribution around cavitation bubble in the collapsing process. When incident shock wave impacts on the bubble the shock wave is diffracted around bubble and it propagates toward downstream. Due to the pressure difference between back and forth of shock plane, the bubble is asymmetrically contracted with concave shape. At this time, a sort of microjet is formed and eventually it impinges on the rear surface of the bubble with reflection shock wave as shown in Fig.5.

And then, present numerical method applied to shock-bubble interaction problems between stationary or

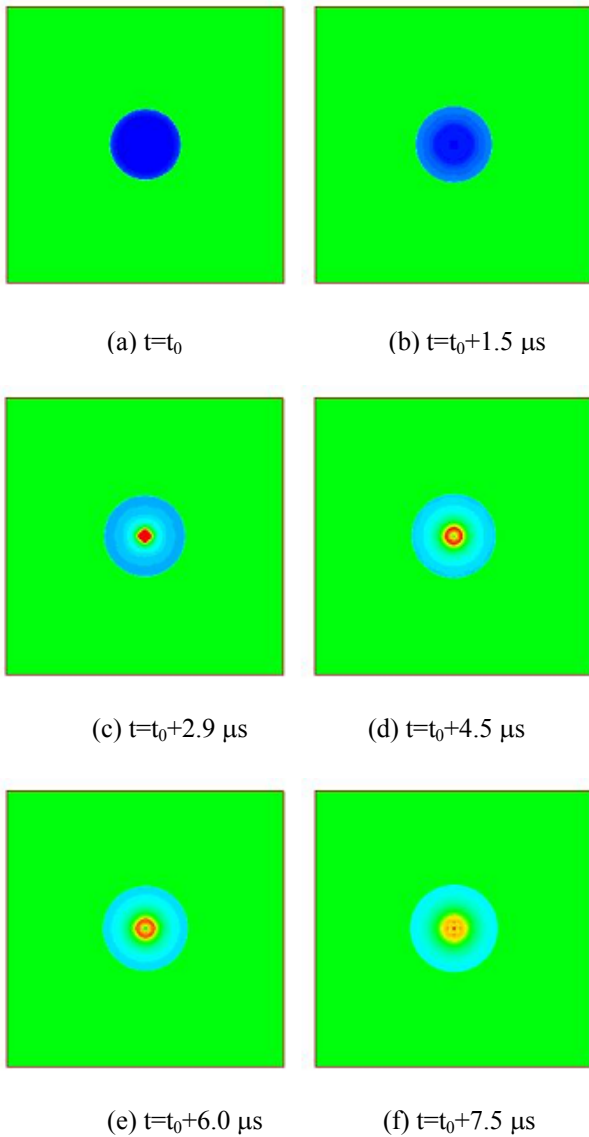


Figure 6 Collapse of a bubble in a hydrostatic pressure field and a rebound
(red: 240MPa, Green: 10MPa, blue: 0.1MPa)

incident liquid shock wave and cylindrical cavitation bubbles located in the liquid. Previous square domain and grid points are used. As an initial condition, a single bubble with void fraction of $\alpha=1$ is located in the center of a stationary flow field with $\alpha=0$ at isothermal condition. The initial pressure of gas in bubble was taken as 0.1MPa. A uniform pressure of 10MPa was given around the bubble. Figure 6 shows a time evolution of bubble collapsing process. Bubble is gradually shrunken by the initial pressure difference up to almost terminal stage of collapse. At this time pressure in the bubble reaches maximum value around 240MPa and a rebound shock wave occurs. Then this wave propagates to liquid region and the bubble is expanded with time. Bubble collapsing behavior, shock-bubble interaction and shock transmission /reflection pattern are well simulated in this application.

5 CONCLUSIONS

A high resolution numerical method for gas-liquid two-phase flow with variable density is applied to solve shock tube and shock-bubble interaction problems. In the proposed method, a finite-difference 4th-order Runge-Kutta method combined with MUSCL TVD scheme is employed, and a homogeneous equilibrium model of gas-liquid two-phase flows is applied. From the numerical example of gas-liquid two-phase 1-D shock tube problems, it is confirmed that the present high resolution numerical method quite well simulates unsteady phenomena of the shock waves with contact discontinuity. It showed a successive application to two-phase shock tube flows, and a good prediction of pressure, density, velocity and void fraction distributions in comparison with exact solutions. At shock-bubble interaction problems between cylindrical single cavitation bubble located in the liquid and incident liquid shock wave, bubble collapsing behavior is investigated and shock-bubble interaction and shock transmission/reflection pattern are well simulated.

ACKNOWLEDGEMENTS

A part of this research is financially supported by Underwater Vehicle Research Center (UVRC), DAPA of Korea.

REFERENCES

- Beattie, D.R.H., and Whally, P.B. (1982). 'A Simple Two-Phase Frictional Pressure Drop Calculation Method.' *Int. J. Multiphase Flow*, **8**, pp.83-87.
- Bourne, N.K. & Field, J.E. (1992). 'Shock-Induced Collapse of Single Cavities in Liquids,' *J. of Fluid Mech.*, **244**, pp.225-240.
- Brennen, C.E. (1995). *Cavitation and Bubble Dynamics*. Oxford Univ. Press.
- Chen, H.T., and Collins, R. (1971). 'Shock Wave Propagation Past on Ocean Surface.' *J. Comput. Phys.* **7**, pp.89-101.
- Chen, Y. & Heister, S.D. (1994). 'A Numerical Transfer for Attached Cavitation.' *ASME J. Fluid Engng.* **116**, pp.613-618.
- Deshpande, M., et al. (1997). 'Numerical Modeling of the Thermodynamic Effects of Cavitation,' *ASME J. of Fluids Eng.* **119**, pp.420-427.
- Iga, Y., et al. (2003). 'Numerical Study of Sheet Cavitation Break-off Phenomenon on a Cascade Hydrofoil.' *ASME J. Fluid Engng.* **125**, pp.643-651.
- John, J.E.A. (1984). 'Gas Dynamics.' Allyn and Bacon, Inc., Boston.
- Kunz, R.F., et al. (2000). 'A Preconditioned Navier-Stokes Method for Two-Phase Flows with Application to Cavitation Prediction,' *Computers & Fluids*, **29**, pp.849-875.
- Laney, C.B. (1998). 'Computational Gasdynamics.' Cambridge Univ. Press, Cambridge.

- Merkle, C. L., et al. (1998). 'Computational Modeling of the Dynamics of Sheet Cavitation,' Proc., 3rd Int., Sympo. on Cavitation, **2**, pp.307-311.
- Roe, P.L. (1981). 'Approximate Riemann Solvers, Parameter Vectors and Difference Scheme.' J. Comp. Phys. **43**, pp.357-372.
- Shin, B.R. (2001). 'Numerical Analysis of Unsteady Cavitating Flow by a Homogeneous Equilibrium Model.' 31st AIAA Fluid Dyn. Conf., AIAA Paper 2001-2909.
- Shin, B.R., et al. (2003), 'A Numerical Study of Unsteady Cavitating Flows Using a Homogenous Equilibrium Model.' Computational Mechanics, **30**, pp.388-395.
- Shin, B.R., et al. (2004). 'Application of Preconditioning Method to Gas-Liquid Two-Phase Flow Computations.' ASME J. Fluid Engng., **126**, pp.605-612.
- Shin, B.R. & Ikohagi, T. (1999). 'Numerical Analysis of Unsteady Cavity Flows Around a Hydrofoil.' ASME Paper FEDSM 99-7215.
- Shin, B.R. and Yamamoto, S. (2005). 'A Preconditioning Method for Two-Phase Flow with Cavitation.' Computational Fluid Dynamics Journal, **13**, pp.722-729.
- Singhal, A. K. et al. (1997). 'Multi-Dimensional Simulation of Cavitating Flows Using a PDF Model for Phase Change,' ASME Paper FEDSM97-3272.
- Takahira, H., et al. (1994). 'Numerical Analysis of Interaction between Single Bubble and Shock Wave,' Trans. JSME B, **60**, pp.2976-2983.
- Tomita, T. & Shima, A. (1986). 'Mechanisms of Impulsive Pressure Generation and Damage Pit Formation by Bubble Collapse,' J. of Fluid Mech., **169**, pp.535-564.
- van Leer, B. (1979). 'Towards the Ultimate Conservative Difference Scheme V. A Second-Order Sequel to Godunov's Method.' J. Comput. Phys. **32**, pp.101-136.
- Yamamoto, S. and Shin, B.R. (2004). 'A Numerical Method for Natural Convection and Heat Conduction around and in a Horizontal Circular Pipe.' Int'l J. of Heat and Mass Transfer, **47**, pp.5781-5792.